

MICROMIRROR SLM FOR FEMTOSECOND PULSE SHAPING IN THE ULTRAVIOLET

M. Hacker, G. Stobrawa, R. Sauerbrey, T. Buckup, M. Motzkus, M. Wildenhain, A. Gehner

ABSTRACT

We present the application of a novel micro mirror array, which is based on a micro electro mechanical system (MEMS), as one- and two-dimensional phasemodulating spatial light modulator (SLM) for femtosecond pulse shaping in the spectral region from the deep-ultraviolet (DUV) to the near-infrared (NIR) (200–900 nm). Using such a high-resolution MEMS-SLM, we demonstrate one-dimensional pulse shaping at 400 nm.

1 Introduction

Femtosecond pulse shaping [1] has developed into a crucial technology for the coherent control of quantum systems [2,3], as well as for advanced dispersion control [4], nonlinear optics and optical communication [5]. The application of conventional programmable pulse shapers [6–10] is restricted to the visible (VIS) and near infrared (NIR) spectral range because of the limited transparency range of common modulator materials, such as liquid crystals (LC) or TeO₂. Only in a few cases the accessible range exceeds the VIS and NIR, but always at the cost of resolution [11–13]. On the other hand, the availability of shaped pulses in the ultraviolet (UV) and deep ultra violet (DUV) would offer a variety of applications, including new approaches to the control of electronic responses of atoms and molecules.

Therefore effort has been made to extend the accessible spectral range by frequency conversion of shaped pulses [14–16]. However, direct high-resolution pulse shaping in these spectral regions would be more convenient compared to previous techniques. In this paper we propose the application of a novel phase-shifting spatial light modulator (SLM) for pulse shaping by direct Fourier filtering [1] of femtosecond pulses from the DUV to the NIR and demonstrate experimentally one-dimensional pulse shaping at 400 nm. For the SLM considered here, a demonstrator device of a micro-electromechanical system (MEMS) micromirror array was used, which is currently under development for phase-frontcorrecting applications in adaptive optics [17, 18].

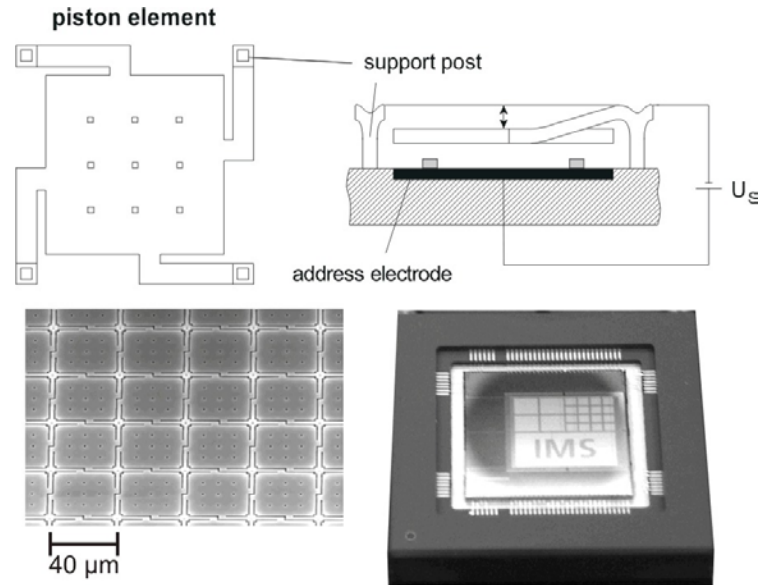


Fig. 1: A schematic top- and side-view of a single piston element of the MEMS-SLM, a scanning electron microscopy (SEM) photograph of the arrayed elements, and a picture of the whole modulator showing a test pattern. Each of the 240×200 piston elements has a size of $40 \times 40 \mu\text{m}^2$ and can perform vertical deflections of 450 nm

The array shown in Fig. 1 consists of independently addressable piston-type micromirrors, which are fabricated by surface-micromachining within a fully CMOS-compatible process on top of an underlying integrated active-matrix address circuitry. The process only needs three additional masks, which easily allows for a modification of the light-modulating properties by simply changing the mirror architecture to meet different application specific requirements. The micromirrors are fabricated in a sacrificial-layer technique, forming free-standing mirror elements over an air gap with an underlying address electrode. Mirrors and support posts are both made of an aluminium alloy, ensuring a high reflectivity in a wide spectral range from the DUV to the NIR. The device is activated by applying a signal voltage between the mirror and the address electrode, which causes the mirror to deflect into the air gap due to the acting electrical field forces. The incident light then undergoes a phase modulation according to the optical path differences given by the programmed overall deflection pattern. Since the maximum vertical deflection of one mirror element is about 450 nm, phase modulations of $0-2\pi$ can be performed for wavelengths shorter than 900 nm. The spectral limit towards shorter wavelengths of about 200 nm mainly arises from the reflectivity of the aluminium alloy and also from the surface planarity of the micromirrors, which is currently on the order of 10 nm (RMS). In contrast with LC modulators, the phase modulation performed by a MEMS mirror device is independent from the polarization state of light under perpendicular incidence. While the mechanical switching time of one mirror element is about $10 \mu\text{s}$, one complete programming cycle of the CMOS address matrix takes about 1ms, which corresponds to an image repetition rate of 1 kHz [17, 18]. Because of the two-dimensional arrangement of the elements, these modulators are superior devices for two-dimensional pulse shaping [19]. Practicable pixel sizes are in the range of $40 \times 40 \mu\text{m}^2$ and above. To demonstrate the applicability of these modulators under typical conditions the aforementioned demonstrator device with 240×200 elements was adopted for pulse shaping of

femtosecond pulses at 404 nm, including generation of THz-pulse sequences by sinusoidal phase-modulation and pre-compensation of the group velocity dispersion (GVD) of a glass rod. Regarding the one-dimensional character of the required deflection patterns, all elements in each column were addressed equally. Thereby, the available 8-bit address resolution corresponding to a phase shift resolution of less than 12 nm, as well as the overall reprogramming rate of 100 Hz, is currently determined by the controller device of the MEMS-SLM, but will be increased to the kHz-level in the future.

2 Experimental setup

Figure 2 shows the experimental arrangement: a Ti:Sapphire laser with amplifier delivers pulses with a center wavelength of 808 nm, 27 nm bandwidth and about 50 fs duration (FWHM) at a power level of 800 μ J and a repetition rate of 50 Hz. The pulses were divided by a beamsplitter into two fractions; the first ($\approx 40\%$) is frequency doubled in a 100 μ m-thick BBO crystal and the second ($\approx 60\%$) is sent into a delay line as the reference pulse. The second harmonic radiation has a pulse energy of about 2 μ J, a bandwidth of 7 nm (FWHM), and a beam diameter of about 5mm, which is determined by the crystal aperture. Then, the second harmonic is reflected by a dichroic mirror to suppress the fundamental radiation. These UV pulses are sent onto an aluminium-coated diffraction grating (2400 lines per mm), which results in an angularly dispersed spectrum. The spectrum is focused onto the MEMS-SLM using a fused-silica cylindrical lens with a focal length of $f = 57$ mm. Since the distance between the grating and the lens and between the lens and the MEMS-SLM are equal, these three optical elements act as a folded 4-f zerodispersion compressor with a phase modulator in the Fourier plane [1]. The phase-modulation is provided by the deflection pattern of the MEMS-SLM and is refreshed for each impinging laser pulse. For this first demonstration, the second harmonic spectrum illuminated only about one third of the SLM due to the currently available optics. Nevertheless, full illumination, i.e. optimal performance, could be achieved easily by refining the focal length or the grating dispersion. After reflection and phase-modulation by the MEMS-SLM, the pulses leave the shaper by passing its elements in reverse order. By slightly tilting the SLM perpendicular to the spectral plane one achieves separation of the outgoing beam from the incoming at the shaper output. The MEMS-SLM within the pulse shaper has a high reflection efficiency of about 85% for the second harmonic pulses, which makes this device ideal for pulse shaping in the UV. The discrepancy between this reflection efficiency and the reflectivity of the mirror material of about 90% is attributed to diffraction losses resulting from the gaps between adjacent mirrors (see Fig. 1) representing a permanent two-dimensional grating structure. Using a second dichroic mirror the shaped UV pulses are superposed collinearly with the delayed fundamental reference pulse in a second 100- μ m thick BBO crystal without focusing to generate third harmonic radiation (THG) as the cross-correlation signal. After spectral separation by a fused silica prism this signal is detected by a silicon carbide photo diode.

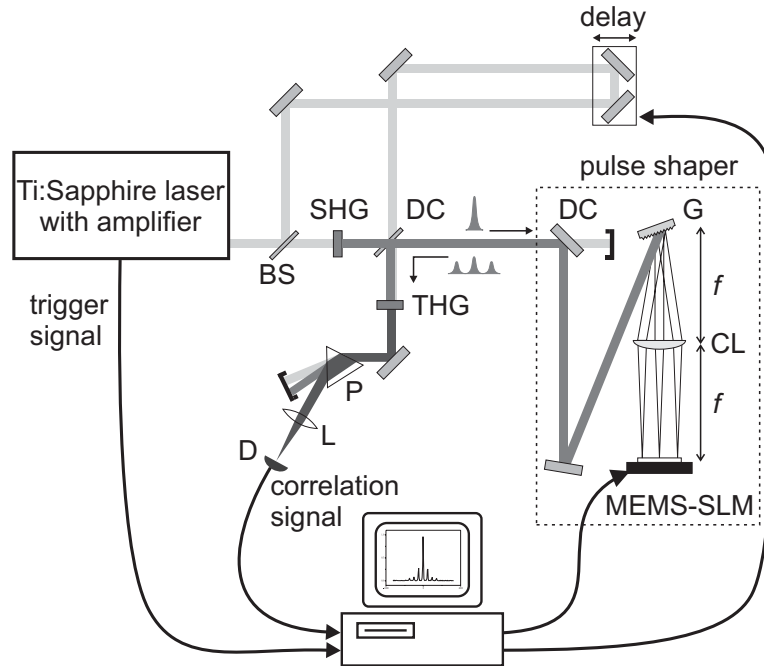


Fig. 2: Experimental setup: BS, beamsplitter; CL, cylindrical fused silica lens ($f = 57$ mm); DC, dichroic mirror; D, detector; G, diffraction grating (2400 lines/mm); L, fused silica lens; MEMS-SLM, micro-electro-mechanical spatial light modulator; P, prism; SHG, second harmonic generation in a 100- μm BBO; THG, third harmonic generation in a 100- μm BBO

3 Results

As an initial test, the second harmonic spectra before and after the pulse shaper were compared and it was found that no spectral alterations appeared, whether the modulator was active or not. In a second step, the temporal structure of the UV pulses after passage through the pulse shaper was investigated by cross-correlation with the delayed reference pulses.

Figure 3a shows the cross-correlation trace for the inactive modulator. The trace has a FWHM of about 80 fs, showing that the intrinsic residual dispersion of the shaper is reasonably small for most applications. At ± 1.94 ps, replicas of the pulse appear that are attributed to the influence of the gaps between adjacent mirror elements and are known from liquid crystal arrays. The position of these replicas mark the edges of the effective sinc²-shaped time window accessible for the shaper with the given parameters [20]. This time window can be easily tripled by optimized illumination of the active area of the SLM.

As a typical application of a pulse shaper, different THz-pulse trains were generated by applying sinusoidal phase-modulations (Fig. 3b–d). The temporal separations within the pulse trains are in excellent agreement with the theoretically expected values for the applied sinusoidal phase modulations. In addition, the position and shape of the replicas in Fig. 3 change with the modulation frequency. This can be explained by the fact that the replicas are also subject to the pulse train generation. Therefore, parts of these pulse train replicas are shifted towards the center of the sinc-shaped time window mentioned above [20], which results in an increase of their amplitudes.

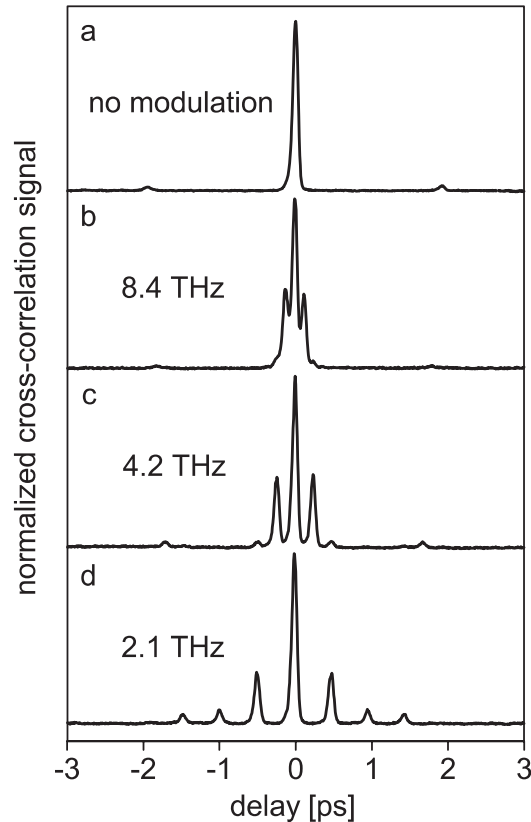


Fig. 3: Measured cross-correlation traces of UV pulses resulting from the inactive modulator (a) and from the modulator performing sinusoidal phase-modulations with an amplitude of $\pi/2$ and periods of 16, 8, and 4 pixels (b–d). The generated THz-pulse trains have theoretical repetition rates of b $(119 \text{ fs})^{-1} = 8.4 \text{ THz}$, c $(238 \text{ fs})^{-1} = 4.2 \text{ THz}$, and d $(476 \text{ fs})^{-1} = 2.1 \text{ THz}$

4 Conclusion

In conclusion, the use of a novel MEMS-type SLM for high resolution pulse-shaping has been presented [22] and its feasibility for pulse shaping in the UV at 400 nm has been demonstrated. The MEMS-SLM possesses a high reflectivity from the NIR down to the DUV (900–200 nm), a high image repetition rate of $> 1 \text{ kHz}$, and is insensitive to the polarization of the incident light. The current spatial resolution of 240×200 pixels is comparable to that of commercially available high resolution LC-SLM [19, 20, 21]. Due to the capability to create directly shaped ultraviolet complex pulses, the application of the novel MEMS-type SLM paves the way for coherent control experiments on important organic chemical and biological compounds, which typically have absorption spectra below 400 nm.

- [1] A.M. Weiner: *Rev. Sci. Instrum.* 71, 1929 (2000)
- [2] H. Rabitz, R. de Vivie-Riedle, M. Motzkus, K. Kompa: *Science* 288, 824 (2000)
- [3] S. Rice, M. Zhao: *Optical Control of Molecular Dynamics* (John Wiley, New York 2000)
- [4] M. Hacker, G. Stobrawa, R. Sauerbrey: *Opt. Lett.* 28, 209 (2003)

- [5] Z. Zheng, A.M. Weiner: *Opt. Lett.* 25, 984 (2000)
- [6] A.M. Weiner, D.E. Leaird, J.S. Patel, J.R. Wullert: *Opt. Lett.* 15, 326 (1990)
- [7] M.M. Wefers, K.A. Nelson: *Opt. Lett.* 20, 1047 (1995)
- [8] C.W. Hillegas, J.X. Tull, D. Goswami, D. Strickland, W.S. Warren: *Opt. Lett.* 19, 737 (1994)
- [9] D.E. Leaird, A.M. Weiner: *Opt. Lett.* 24, 853 (1999)
- [10] F. Verluise, V. Laude, Z. Cheng, C. Spielmann, P. Tournois: *Opt. Lett.* 25, 575 (2000)
- [11] E. Zeek, K. Maginnis, S. Backus, U. Russek, M. Murnane, G. Mourou, H. Kapteyn, G. Vdovin: *Opt. Lett.* 24, 493 (1999)
- [12] G. Vdovin, M. Loktev: *Opt. Lett.* 27, 677 (2002)
- [13] A. Suda, Y. Oishi, K. Nagasaka, P. Wang, K. Midorikawa: *Opt. Express* 9, 2 (2001)
- [14] M. Hacker, T. Feurer, R. Sauerbrey, T. Lucza, G. Szabo: *J. Opt. Soc. Am. B* 18, 866 (2001)
- [15] T. Witte, D. Zeidler, D. Proch, K.L. Kompa, M. Motzkus: *Opt. Lett.* 27, 131 (2002)
- [16] H.-S. Tan, E. Schreiber, W.S. Warren: *Opt. Lett.* 27, 439 (2002)
- [17] A. Gehner, W. Doleschal, A. Elgner, R. Kauert, D. Kunze, M. Wildenhain: *Proc. SPIE* 4561, 265 (2001)
- [18] A. Gehner, M. Wildenhain, W. Doleschal, A. Elgner, H. Schenk, H. Lakner: *Proc. SPIE* 4983, 180 (2003)
- [19] T. Feurer, J.C. Vaughan, R.M. Koehl, K.A. Nelson: *Opt. Lett.* 27, 652 (2002)
- [20] M.M. Wefers, K.A. Nelson: *J. Opt. Soc. Am. B* 12, 1343 (1995)
- [21] G. Stobrawa, M. Hacker, T. Feurer, D. Zeidler, M. Motzkus, F. Reichel: *Appl. Phys. B* 72, 627 (2001)
- [22] *Appl. Phys. B* 76, 711–714 (2003)